The Saudi Dental Journal (2023) **35**, 819–826

King Saud University

The Saudi Dental Journal

www.ksu.edu.sa
www.sciencedirect.com

ORIGINAL ARTICLE

Effect of controlled surface roughness and biomimetic coating on titanium implants adhesion to the bone: An experiment animal study

Mohamed Ahmed Alkhodary *

Department of Prosthetic Dental Sciences, College of Dentistry, Qassim University, Saudi Arabia
Faculty of Dentistry, Alexandria University, Egypt

Received 27 April 2023; revised 8 July 2023; accepted 10 July 2023
Available online 16 July 2023

KEYWORDS

Laser micro-grooving;
RGD coating;
Titanium implants;
White New Zealand rabbits;
Mechanical testing

Abstract *Introduction:* Laser micromachining of titanium and its alloys can create micro-grooves with sizes similar to cell diameter of about 10 μm. Its coating with arginine-glycine-aspartic acid (RGD) may enhance cellular spreading and adhesion. This study aimed to evaluate the effect of laser micro-grooving and laser micro-grooving combined with RGD coating on the strength of the dental implants/bone interface using destructive mechanical pullout testing in experimental animals.

Materials and methods: In this study, the test groups consisted of 1.5-mm diameter, 5-mm long laser-grooved and laser-grooved/RGD coated titanium alloy (Ti–6Al–4 V) rods, and the control group included plain titanium alloy (Ti–6Al–4 V) rods. These rods were implanted in the mandibles of New Zealand white rabbits for 2, 4, and 6 weeks. After sacrifice, the test and control specimens were retrieved for mechanical pullout testing. The DMA 7-e was used to pull the titanium rods out of the bone, the probe position was plotted versus time graph to monitor the test progression, and the static modulus versus time graph was viewed; such graphs was then transformed into tables. The results were analyzed using the Mann-Whitney test.

Results: The laser-grooved/RGD coated rods had significantly higher pull-out strength than the laser-grooved and control rods. Additionally, the laser-grooved rods had significantly higher pull-out strength than control rods.

Conclusion: Two novel surface treatments were used: laser micro-grooving and tri peptide RGD coating, both of which had different effects on the dental implant interface. Laser grooving

* Corresponding author at: Department of Prosthetic Dental Sciences, College of Dentistry, Qassim University, P.O. Box 6700, Burydah 51452, Saudi Arabia.
E-mail address: dr.mohamed.alkhodary@qudent.org.

Peer review under responsibility of King Saud University.

ELSEVIER Production and hosting by Elsevier

https://doi.org/10.1016/j.sdentj.2023.07.010

improved *peri*-implant bone healing, whereas RGD coating facilitated earlier bone–implant adhesion and better mineralization.

1. Introduction

In laser micromachining, the surface of titanium and its alloys can be modified by laser, creating micro-grooves with a size in the order of a cell diameter of about 10 µm, which promotes better interaction between the surface and the surrounding environment. However, there are considerable variations in the literature regarding the effects of micro-groove geometry on cell orientation and integration with titanium surfaces (Dee and Puleo, 2000; Anselme, 2000; Wilson et al., 2005; Sader et al., 2005; Huang et al., 2004; Wang et al., 2000; Ricci and Alexander, 2001). Consequently, the production of a dental implant with controlled surface roughness was considered to facilitate basic studies on the effects of laser groove dimensions and geometry on cell adhesion to titanium surfaces (Chen et al., 2011; Farronato et al., 2014; Veiko et al., 2021; Alkhodary, 2014; Zheng et al., 2022; Chen et al., 2009; Mastrangelo et al., 2020).

The Arg-Gly-Asp peptide (RGD peptide) immobilized on titanium surfaces serve as a molecular bridge for enhancing the adhesion of bone-forming cells to titanium dioxide implant surfaces, which in turn improves the mechanical properties of the developing bone–implant interface (Morra, 2006; Rezania and Healy, 2000; Kroese-Deutman et al., 2005; Elmengaard and Bechtold, 2005; Parfenov et al., 2019; Xu and Jiang, 2022; Xu et al., 2022; Heller et al., 2018 Feb; Dayan et al., 2019; Syam et al., 2021; Georgieva et al., 2023; Chen et al., 2022; Onak et al., 2018). The synergistic osteogenesis resulting from the bioinspired peptide RGD adhesion on Ti implants has been found to alleviate wear particle-induced inflammation and promote interfacial osteogenesis (Syam et al., 2021; Georgieva et al., 2023; Chen et al., 2022; Onak et al., 2018; Ma et al., 2022; Guo et al., 2022; Zhou et al., 2019; Wang et al., 2013; Fu et al., 2009; Bly et al., 2007; Milburn et al., 2009; Alkhodary et al., 2010; Marei et al., 2010 Jan; Salifu et al., 2020; Salifu et al., 2020).

Pushout and pullout tests are commonly employed to assess the ex-vivo mechanical competence of biological fixation in orthopedic and dental implants by evaluating the shear strength of the bone–implant interface. These tests are widely used due to their relatively simple test protocols, typically involving a uniaxial material testing machine operated under displacement control, along with a simple support jig for the pushout test or a hookup system for the pullout test (Pitzen et al., 2004; Lawson and Brems, 2001; Reitman et al., 2004; Koistinen et al., 2003; Park and Kwon, 2004; Liebschner, 2004; International Standard ISO 10993-6, 1994; Neyt et al., 1998; Shirazi-Adl et al., 1994; Berzins et al., 1997; Benesch et al., 2008; Schwartz et al., 2003; Mavrogenis et al., 2009; Joos et al., 2006; Hansson, 1999; Marco et al., 2004; Steven et al., 2006; Jaasma et al., 2002).

Based on the aforementioned data, this study aimed to evaluate the effect of laser micro-grooving and the combined laser micro-grooving/RGD coating on the dental implant/bone interface strength in experimental animals using destructive mechanical pullout testing.

2. Materials and methods

In this study, 1.5-mm diameter, 5-mm-long laser-grooved and laser-grooved/arginine-glycine-aspartic acid (RGD) coated titanium alloy (Ti–6Al–4 V) rods were used as the test group, and the control group consisted of plain titanium alloy (Ti–6Al–4V) rods. These rods were implanted in the mandibles of New Zealand white rabbits for 2, 4, and 6 weeks. The animals were then sacrificed, and the test and control specimens were retrieved for mechanical pullout testing.

2.1. Laser micro-grooving of the titanium implants

The coherent AVIA laser machine (AVIA 355–4500) was used for the laser grooving process. The AVIA is a pulsed laser, in contrast to a continuous wave laser, in which the output only occurs in bursts every time the laser is triggered. The AVIA was set up to output 40 ns pulses at a wavelength of 355 nm in the ultraviolet spectrum (Fig. 1). After setting the AVIA laser machine to work on external mode, with the laser beam pulsed with every 20-µm movement of the Aerotech stage, the titanium rods were laser micro-grooved as follows:

- The titanium rods, provided by McMaster Carr, Inc., were initially reduced in diameter from 4 to 1.5 mm using a traditional milling machine (Hardinge Brothers, Inc.).
- Two titanium rods with a diameter of 1.5 mm and length of 24 mm were joined together using heat shrink tubes (McMaster Carr, Inc.).
- The setup consisted of a small x-y stage screwed to the Aerotech stage, a specially designed holder fixed to the x-y stage by means of two columns, and a rotation (U or R) stage screwed to the Aerotech stage facing the holder.

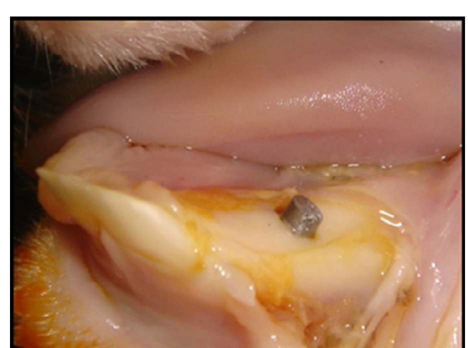

Fig. 1 Surgical site preparation and placement of the titanium rod.

- One of the titanium rods was fixed to the U stage to transfer the rotation to the other rod, which rotated through the holder in an ax-symmetric manner without any off-axis runout.
- The laser micro-grooving was examined using a scanning electron microscope (Philips, Xl30 Feg, Xl Series).

2.2. RGD coating of the titanium implants after laser micro-grooving

- The titanium rods were immersed in a solution of 3 mg 11-hydroxyundecylphosphonate (AP) in 100 ml of tetrahydrofuran (THF; Sigma Aldrich, Batch # 11972ch). The immersion was carried out under continuous stirring conditions until evaporation. Subsequently, the rods were baked for 24 h at 120 °C under vacuum (Isotemp Vacuum Oven, 280a, Fisher Scientific) to form ether bonds between the oxide layer and AP.
- Afterward, the rods were immersed in a solution of 10 mg maleimide (Sigma Aldrich, BATCH #CAS 55750–62-4) in 500 ml of anhydrous acetonitrile (Sigma Aldrich, Batch # 03735hh) in a dry nitrogen chamber under stirring conditions for 24 h.
- Next, the titanium rods were immersed in a solution of 0.5 mg of RGDC (American Peptide Company Inc.) dissolved in 500 ml of distilled water. The reaction between AP and maleimidopropionic acid resulted in the attachment of the R-G-D-C chain to cysteine via addition reactions.
- Fourier Transform Infrared (FT-IR) spectroscopy was employed to verify the success of the RGD coating process. This technique uses a Michelson interferometer to create a beam of light with different frequencies at once. Then, by measuring the absorbed portion of the beam, an interferogram is constructed as the raw signal to detect the infrared emission of the functional RGD groups attached to the surface via the alkyl phosphonate (AP) linker molecule, which would emit different colors at different micro-groves locations when subjected to infrared radiation.

2.3. The experimental animal study

A total of 36 white New Zealand rabbits, 3 months old and weighing 1.5 kg, were used in the study. The sample size was determined using power analysis of sample size, and the study received ethical approval from the College of Dentistry at Alexandria University in Egypt.

The animals were divided into two groups:

- Group I: This group included 18 rabbits, where the right side of each rabbit's mandible received a laser-grooved titanium rod, and the left side received a plain titanium rod as a control.
- Group II: This group included 18 rabbits, where the animals received laser-grooved/RGD coated rods in the right side of their mandibles and plain titanium rods as controls in the left side.

The animals were operated upon under general anesthesia. A crestal incision was made, followed by raising a full-thickness flap to expose the alveolar bone. A 1.2-mm drill was used to establish an osteotomy of 1.5 mm in diameter and 5 mm in depth using a contra-angle handpiece with a reduction speed of 20:1. The implant was manually secured in place using a needle holder (Fig. 1). The tension-free flap was repositioned and sutured. At 2, 4, and 6 weeks following implantation, six animals from each group were sacrificed.

2.4. Ex-vivo testing

After sacrificing the animals, the samples were retrieved. In the presence of a water coolant, a diamond disk was used to cut excess bone mesial and distal to the pin, ensuring that the mesio-distal length of the bone sample was at least three times that of the pin to avoid the end-effect stresses during testing.

A dynamic mechanical analyzer (DMA 7-e, Berkin Elmer, USA) with a maximum tension of 6000 mN was used. Proper vertical orientation of the pin within the sample was crucial to avoid catching effects and concerns about potential misalignment between the implant axis and pullout force. To achieve this, a flat seat was created by cutting the inferior border of the sample. The embedded part of the implant (1 mm) was grasped by the upper member of the DMA 7-e, while the bone retaining the embedded part was grasped by the lower member. A constantly increasing static force was applied, starting with 100 mN and increasing at a rate of 500 mN/min until reaching 6000 mN, in order to pull the titanium pin out of the bone (Fig. 2). The machine generated a graph for each test, which was then transformed into a table (Fig. 3).

2.5. Statistical analysis

Normality was not detected in the studied groups, and since a continuous level variable was measured for all observations, it was necessary to test if the distribution of this variable differed between the groups. The Mann-Whitney test was used to compare between the groups, and the Wilcoxon signed ranks test

Fig. 2 A. Mechanical characterization of the ex-vivo sample using the Dynamic Mechanical Analyzer (DMA 7-e): sample mounted: showing the bone attached to the lower member and the pin attached to the upper member of the assembly, titanium rod pulled-out of place,

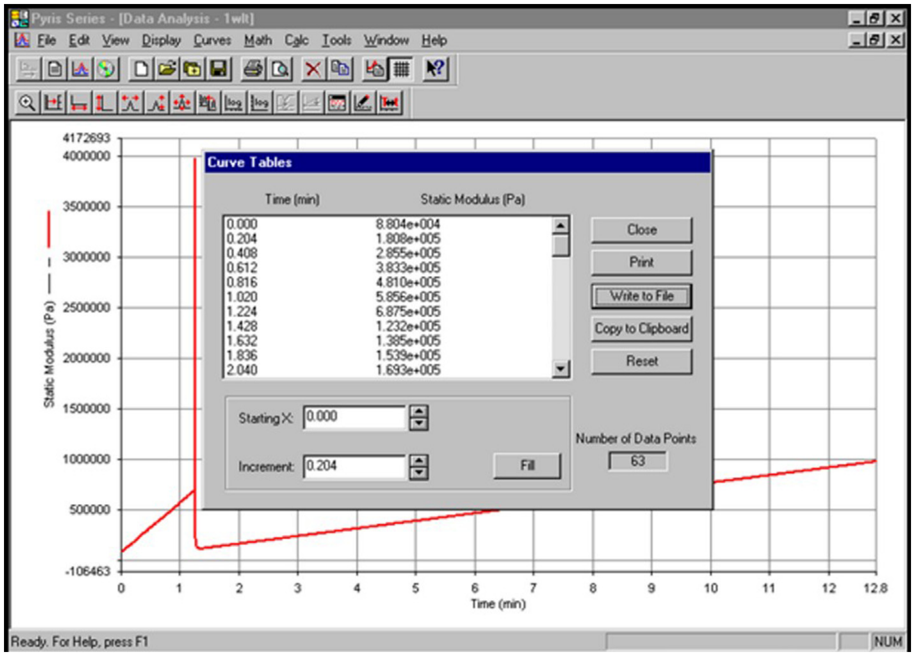

Fig. 3 Transforming the DMA curves into tables: plotting static modulus versus time, and transforming static modulus curve into numerical values for analysis.

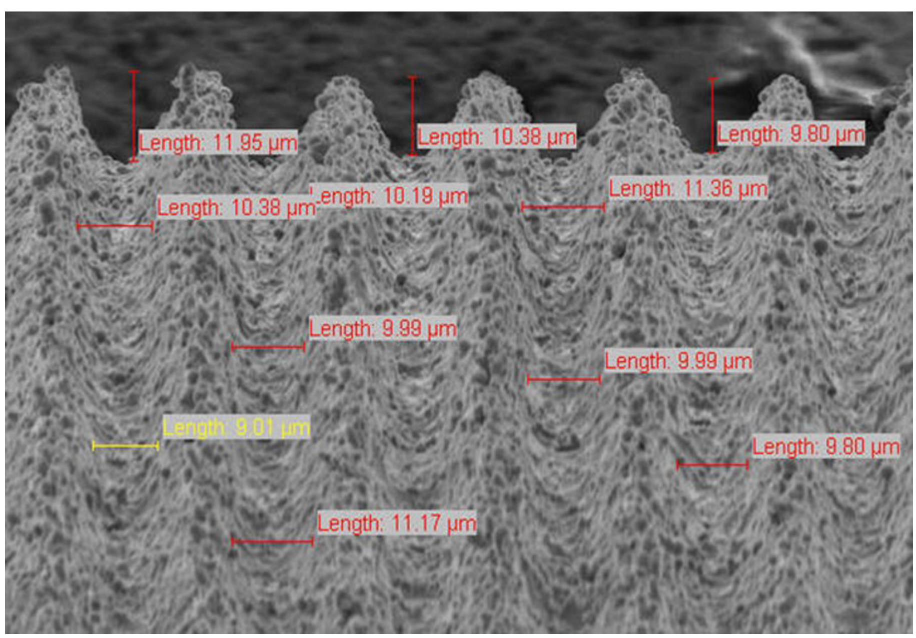

Fig. 4 SEM examination of laser micro-grooves on the titanium rod, note an average depth and width of about 10 um.

was used to assess progress within different time intervals as these tests are commonly employed two-sample nonparametric statistical tests and share similar hypotheses.

3. Results

The SEM study revealed that the engraved micro-groves were of an average width of 10 µm (Fig. 4), and the FT-IR the immunofluorescence showed success of AP linker molecule attachment to the titanium surface through the green and red fluorescence, which was further confirmed by the immunofluorescence curve at about 2750.

- As the DMA 7-e was used to pull the titanium rods out of the bone, the probe position versus time graph provided insights into the test progression, while the static modulus versus time graph allowed for a comparison between the

Table 1 Statistical analysis of the mechanical pull-out results (Pa).

	RGD	Control	Laser
Week 2		–	
Range	67,300 – 4,730,000	–	–
Mean ± SD	2383687.3 ± 1383549.3	–	–
Median	2,380,000		–
Z_1 (p)		–	–
Z_2 (p)			–
Week 4			
Range	89300–3020000	90700–6565000	74300–5480000
Mean ± SD	1141877.8 ± 747835.7	257400.0 ± 1875143.2	2715211.1 ± 1609160.4
Median	846,000	3,165,000	2,690,000
Z_1 (p)		5.750* (< 0.001)	5.528* (< 0.001)
Z_2 (p)			7.829* (< 0.001)
Week 6			
Range	86700–5750000	73200–968000	65700–4910000
Mean ± SD	2982788.9 ± 1665848.9	512701.6 ± 258604.8	2036550.8 ± 1450204.7
Median	2,870,000	493,000	2,430,000
Z_1 (p)		5.103* (< 0.05)	5.503* (< 0.033)
Z_2 (p)			2.430* (< 0.015)

Z_1: for Mann Whitney test between RGD and other groups.
Z_2: for Mann Whitney test between control and laser.
* Statistically significant at $p \leq 0.05$.

groups. These graphs were transformed into tables for statistical analysis using the Mann-Whitney test (Table 1 and Fig. 5):

- At week 2, the laser-grooved/RGD coated rods demonstrated significantly higher strength than the laser-grooved and control rods. The laser-grooved and control rods were too weak to be tested.
- At week 4, the laser-grooved rods exhibited the highest static modulus among the three groups, and there was a statistically significant difference between the groups.
- At week 6, the laser-grooved/RGD rods had the highest static modulus, and the laser group rods was statistically stronger than the control group rods.

The Wilcoxon signed ranks test was used to evaluate the progress within each experiment interval (Table 1 and Fig. 5):

- For laser-grooved/RGD rods: From week 2 to week 4, there was a significant decrease in static modulus values, whereas from week 4 to week 6, there was a significant increase.
- For control plain rods: From week 2 to week 4, there was no statistically significant increase in strength, whereas from week 4 to week 6, there was a significant increase.
- For laser-grooved rods: From week 2 to week 4, there was a significant increase in static modulus values, whereas from week 4 to week 6, there was no statistically significant difference in the pullout strength.

4. Discussion

Laser micro-grooving of dental implants has been successfully applied in clinical applications. Farronato et al. (Farronato et al., 2014) employed laser micro-grooving on the implant neck module in single tooth replacements using immediate loading. Chen et al. (Chen et al., 2011) reported that titanium (Ti-6Al-4V) possesses the necessary biocompatibility and mechanical

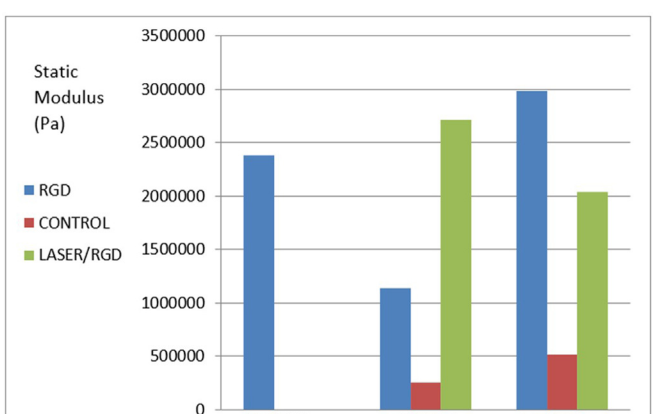

Fig. 5 Mechanical pull-out static modulus mean values for the laser grooved/RGD coated, control, and laser grooved rods at 2, 4, and 6 weeks.

strength for dental implants, with the only drawback being the modulus mismatch with the bone, which calls for the development of new strategies to minimize stress shielding phenomena and enhance the bone–implant interface strength across the entire implant surface, which would reduce the risk of recruiting more aluminum to the surface and associated cytotoxicity compared with any other surface roughening technique.

As shown in the work of Fu et al, (Fu et al., 2009) Bly et al; (Bly et al., 2007) and Milburn et al., (Milburn et al., 2009) the method described in this work to coat titanium surface with RGD gave a chemically bound surface coat that resisted removal by solvent or mechanical methods. This RGD biomimetic coat was also studied by Marei et al. (Marei et al., 2010) and Chen et al. (Salifu et al., 2020) in experimental animal models who reported its success in increasing the bone adhesion; additionally, in a clinical trial by Alkhodary et al., (Alkhodary et al., 2010) which was followed by 5 years of follow-up, (Alkhodary, 2014) and also reported clinical success of RGD coated human dental implants.

Taking into considerations the previous claims about the use of laser grooving and RGD coating, we decided to conduct this study using an experimental animal model. A drawback with using rabbits as the animal model for the assessment of implant materials was its size limitation; however, Wang, (International Standard ISO 10993-6, 1994) Neyt, (Neyt et al., 1998) and Liebschner (Liebschner, 2004) stated that rabbits are a very popular choice of species for the testing of implant materials in bone.

At week 2 of the study, mechanical pullout testing revealed that the laser-grooved and control rods were too weak to be tested. In contrast, the laser micro-grooved/RGD coated rods exhibited significantly better attachment to the bone. This finding aligns with the reports of Benesch (Benesch et al., 2008) and Schwartz (Schwartz et al., 2003) who emphasized the importance of RGD in accelerating the healing process and strengthening initial osseointegration.

At week 4, the laser micro-grooved rods demonstrated a higher pull-out static modulus than the laser-grooved/RGD coated group. This discrepancy prompted a closer examination of the biology of osseointegration and bone–implant interface mineralization. According to Mavrogenis (Mavrogenis et al., 2009) and Joos, (Hansson, 1999) the initial mechanical attachment of the implant to the surrounding bone is followed by a remodeling stage, wherein the mechanical behavior of the interface is deferred. In this context, the possible explanation would be that the RGD coating initiated earlier attachment to the surrounding bone by the second week, whereas the laser grooving achieved this attachment by the third week. By the fourth week, the RGD group might have entered the remodeling stage, leading to inferior mechanical properties compared to the laser group. This explanation was potentiated by the findings of the sixth week, during which the RGD group demonstrated a significantly higher pull-out static modulus due to bone maturation, whereas the laser group, just entering the remodeling stage, exhibited significantly weaker properties.

Throughout the study, the control group consistently displayed inferior mechanical behavior, validating the hypothesis that laser grooving and RGD coating improve the process of osseointegration. The superior mechanical performance of the RGD coated rods highlights the role of such cell attachment binding proteins in developing a stronger bone–implant interface.

The success of the experimental animal study motivated researchers to upgrade the work to a human clinical trial, following ethical principles of respect for persons, beneficence, and justice for the participating human subjects. (Hansson, 1999; Marco et al., 2004; Steven et al., 2006; Jaasma et al., 2002).

The same surface treatment and coating used in the animal study were to be used for human dental implants. Moreover, it was necessary to study the dental implant design in order to develop a macro-mechanical shape that, combined with the surface treatment and coating, minimizes the stress shielding phenomenon. Consequently, a completely new dental implant was designed, manufactured, surface laser-grooved, and RGD coated for use in this study.

5. Conclusion

Titanium possesses the necessary biocompatibility and mechanical strength, with the only disadvantage being the modulus mismatch with the bone, which calls for the development of new strategies to minimize the stress shielding phenomena and consequent stronger bone–implant interface. Laser grooving improved *peri*-implant bone healing, whereas RGD coating promoted earlier bone–implant adhesion and improved mineralization.

Ethical statement

I hereby declare that the submitted work entitled (The effect of controlled surface roughness and biomimetic coating on titanium implants adhesion to the bone: an experiment animal study) has been conducted after obtaining institutional approval of the study that included this animal experimental study and a human clinical trial.

Acknowledgments

The author would like to thank professor Wole Soboyejo and professor Mona K. Marei for their help and guidance.

References

Alkhodary, M.A., 2014. Laser micro-grooved, Arginine-Glycine-Aspartic acid (RGD) coated dental implants, a 5 years radiographic follow-up. Int. J. Health Sci. 8, 361.

Alkhodary, M.A., Marei, M.K., Awadalla, M.A., Soboyejo, W., Kadah, Y.M., 2010. A study of the interface strength of dental implants nano-grooved by laser with and without Arginine-Glycine-Aspartic acid (RGD) coating. PDH Thesis, Removable Prosth Depart, Alexandria University.

Anselme, K., 2000. Osteoblast adhesion on biomaterials. Biomaterials 21, 667.

Benesch, J., Mano, J.F., Reis, R., 2008. Proteins and their peptide motifs in acellular apatite Mineralization of scaffolds for tissue engineering. Tissue Eng. 14, 433–445.

Berzins, A., Shah, B., Weinans, H., et al, 1997. Nondestructive measurements of implant–bone interface shear modulus and effects of implant geometry in pullout tests. J. Biomed. Mater. Res. 34, 337.

Bly, R.A., Cao, Y., Moore, W.A., Soboyejo, W.O., 2007. Investigation of the effects of alkane phosphonic acid/RGD coatings on cell spreading and the interfacial strength between human osteosarcoma cells and Ti–6Al–4V. Mater. Sci. Eng. C 27 (1), 83–89.

Chen, J., Ulerich, J.P., Abelev, E., Fasasi, A., Arnold, C.B., Soboyejo, W.O., 2009. An investigation of the initial attachment and orientation of osteoblast-like cells on laser grooved Ti-6Al-4V surfaces. Mater. Sci. Eng. C 29 (4), 1442–1452.

Chen, J., Bly, R.A., Saad, M.M., AlKhodary, M.A., El-Backly, R.M., Cohen, D.J., Kattamis, N., Fatta, M.M., Moore, W.A., Arnold, C. B., Marei, M.K., 2011. In-vivo study of adhesion and bone growth around implanted laser groove/RGD-functionalized Ti-6Al-4V pins in rabbit femurs. Mater. Sci. Eng. C 31 (5), 826–832.

Chen, L., Wang, B., Ren, H., Wu, Y., Lyu, D., Ouyang, Y., Zhang, Q., Yan, Y., 2022. Arg− Gly− Asp peptide functionalized poly-amino acid/poly (p-benzamide) copolymer with enhanced mechanical properties and osteogenicity. Biomat Adv. 133, 112627.

Dayan, A., Lamed, R., Benayahu, D., Fleminger, G., 2019. RGD-modified dihydrolipoamide dehydrogenase as a molecular bridge for enhancing the adhesion of bone forming cells to titanium dioxide implant surfaces. J. Biomed. Mater. Res. A 107 (3), 545–551.

Dee, K.C., Puleo, D., 2000. Engineering materials for biomedical applications. Mater. Today 3, 7–10.

Elmengaard, B., Bechtold, J.E., 2005. Soballe K : In vivo effects of RGD-coated titanium implants inserted in two bone-gap models. J. Biomed. Mater. Res. 75, 249–255.

Farronato, D., Mangano, F., Briguglio, F., Iorio-Siciliano, V., Riccitiello, F., Guarnieri, R., 2014. Influence of Laser-Lok surface on immediate functional loading of implants in single-tooth replacement: a 2-year prospective clinical study. Int. J. Periodontics Restorative Dent. 34 (1), 79–89.

Fu, G., Milburn, C., Mwenifumbo, S., Cao, Y., Oparinde, G.M., Adeoye, M.O., Therialt, C., Beye, A.C., Soboyejo, W.O., 2009. Shear assay measurements of cell adhesion on biomaterials surfaces. Mater. Sci. Eng. C 29 (4), 1293–1301.

Georgieva, S., Todorov, P., Nikolov, S., Dzhambazova, E., Peneva, P., Assenov, B., Pechlivanova, D., 2023. New N-and C-modified RGD-hemorphins as potential biomedical application on Ti-surface materials: Synthesis, characterization and antinociceptive activity. Mol. Divers. 27 (1), 263–280.

Guo, X., Bai, J., Ge, G., Wang, Z., Wang, Q., Zheng, K., Tao, H., Zhang, L., Zhang, H., Wang, D., Zhang, X., 2022. Bioinspired peptide adhesion on Ti implants alleviates wear particle-induced inflammation and improves interfacial osteogenesis. J. Colloid Interface Sci. 1 (605), 410–424.

Hansson, S., 1999. The implant neck: smooth or provided with retention elements: a biomechanical approach. Clin. Oral Implant Res. 10, 394–405.

Heller, M., Kumar, V.V., Pabst, A., Brieger, J., Al-Nawas, B., Kämmerer, P.W., 2018. Osseous response on linear and cyclic RGD-peptides immobilized on titanium surfaces in vitro and in vivo. J. Biomed. Mater. Res. A 106 (2), 419–427.

Huang, H.H., Ho, C.T., Lee, T.H., et al, 2004. Effect of surface roughness of ground titanium on initial cell adhesion. Biomol. Eng 21, 93.

International Standard ISO 10993-6, 1994. Biological evaluation of medical devices 6, pp. 1-11.

Jaasma, M.J., Bayraktar, H.H., Niebur, G.L., et al, 2002. Biomechanical effects of intra specimen variations in tissue modulus for trabecular bone. J. Biomech. 35, 237–246.

Joos, U., Wiesmann, H.P., Szuwart, T., et al, 2006. Mineralization at the interface of implants. Int. J. Oral Maxillofac. Surg. 35, 783–790.

Koistinen, A., Santavirta, S., Lappalainen, R., 2003. Apparatus to test insertion and removal torque of bone screws. Proc. Inst. Mech. Eng. 217, 503–508.

Kroese-Deutman, H.C., Van Den Dolder, J., Spauwen, P.H.M., et al, 2005. Influence of RGD-loaded titanium implants on bone formation in vivo. Tissue Eng. 11, 1867–1875.

Lawson, K.J., Brems, J., 2001. Effect of insertion torque on bone screw pullout strength. Orthop. 24, 451–454.

Liebschner, M.A., 2004. Biomechanical considerations of animal models used in tissue engineering of bone. Biomaterials 25, 1697–1714.

Ma, S., Li, X., Hu, H., Ma, X., Zhao, Z., Deng, S., Wang, J., Zhang, L., Wu, C., Liu, Z., Wang, Y., 2022. Synergetic osteogenesis of extracellular vesicles and loading RGD colonized on 3D-printed titanium implants. Biomater. Sci. 10 (17), 4773–4784.

Marco, V., Mario, D., Fulvia, T., et al, 2004. Automatic generation of accurate subject-specific bone finite element models to be used in clinical studies. J. Biomech. 37, 1597–1605.

Marei, M.K., Saad, M.M., El-Backly, R.M., Al-Khodary, M.A., Bly, R.A., Cohen, D.J., Chen, J., Fata, M.M., Soboyejo, W.O., Nageeb, M., Rashad, A., 2010. Bone engineering around laser grooved RGD-coated titanium surface. Eur. Cells Mater. J. 1 (19), 37.

Mastrangelo, F., Quaresima, R., Canullo, L., Scarano, A., Lo Muzio, L., Piattelli, A., 2020. Effects of novel laser dental implant microtopography on human osteoblast proliferation and bone deposition. Int. J. Oral Maxfac. Imp. 1 (35), 2.

Mavrogenis, A.F., Dimitriou, F., Parvizi, J., et al, 2009. Biology of implant osseointegration. J. Musculoskelet. Neuronal Interact. 2, 61–71.

Milburn, C., Chen, J., Cao, Y., Oparinde, G.M., Adeoye, M.O., Beye, A., Soboyejo, W.O., 2009. Investigation of effects of Argenine–Glycine–Aspartate (RGD) and nano-scale titanium coatings on cell spreading and adhesion. Mater. Sci. Eng. C 29 (1), 306–314.

Morra, M., 2006. Biochemical modification of titanium surfaces: peptides and ECM proteins. Eur. Cell. Mater. 12, 1–15.

Neyt, J.G., Buckwalter, J.A., Carroll, N.C., 1998. Use of animal models in musculoskeletal research. Iowa Orthop. 18, 118–123.

Onak, G., Yurtseven, B., Gökmen, O., Karaman, O., 2018. Comparison the Effect of RGD Peptide Conjugation on Titanium Discs with Different Methods on Cell Adhesion and Proliferation. In: 2018 Medical Technologies National Congress (TIPTEKNO) 2018 Nov 8. IEEE, pp. 1-3.

Parfenov, E.V., Parfenova, L.V., Dyakonov, G.S., Danilko, K.V., Mukaeva, V.R., Farrakhov, R.G., Lukina, E.S., Valiev, R.Z., 2019. Surface functionalization via PEO coating and RGD peptide for nanostructured titanium implants and their in vitro assessment. Surf. Coat. Technol. 15 (357), 669–683.

Park, H.S., Kwon, T.G., 2004. Sliding mechanics with micro-screw implant anchorage. Angle Orthod. 74, 703–710.

Pitzen, T., Franta, F., Barbier, D., et al, 2004. Insertion torque and pullout force of rescue screws for anterior cervical plate fixation in a fatigued initial pilot hole. J. Neurosurg. Spine 1, 198–201.

Reitman, C.A., Nguyen, L., Fogel, G.R., 2004. Biomechanical evaluation of relationship of screw pullout strength, insertional torque, and bone mineral density in the cervical spine. J. Spinal Disord. Tech. 17, 306–311.

Rezania, A., Healy, K.E., 2000. The effect of peptide surface density on mineralization of a matrix deposited by osteogenic cells. J. Biomed. Mater. Res. 52, 595–600.

Ricci, J.L., Alexander, H., 2001. Laser microtexturing of implant surfaces for enhanced tissue integration. Key Eng. Mater. 198–199, 179.

Sader, M.S., Balduino, A., Soares, G.A., et al, 2005. Effect of three distinct treatments of titanium surface on osteoblast attachment, proliferation, and differentiation. Clin. Oral Implant Res. 16, 667.

Salifu, A.A., Obayemi, J.D., Uzonwanne, V.O., Soboyejo, W.O., 2020. Mechanical stimulation improves osteogenesis and the mechanical properties of osteoblast-laden RGD-functionalized polycaprolactone/hydroxyapatite scaffolds. J. Biomed. Mater. Res. A 108 (12), 2421–2434.

Schwartz, J., Avaltroni, M.J., Danahy, M.P., et al, 2003. Cell attachment and spreading on metal implant materials. Mater. Sci. Eng. 23, 395–400.

Shirazi-Adl, A., Dammak, M., Zukor, D.J., 1994. Fixation pullout response measurement of bone screws and porous-surfaced posts. J. Biomech. 27, 1249.

Steven, K., Boyda, B., Ralph, M., 2006. Smooth surface meshing for automated finite element model generation from 3D image data. J. Biomech. 39, 1287–1295.

Syam, S., Wu, C.J., Lan, W.C., Ou, K.L., Huang, B.H., Lin, Y.Y., Saito, T., Tsai, H.Y., Chuo, Y.C., Yen, M.L., Liu, C.M., 2021. The potential of a surface-modified titanium implant with tetrapeptide for osseointegration enhancement. App. Sci. 11, 2616.

Veiko, V., Karlagina, Y., Itina, T., Kuznetsova, D., Elagin, V., Zagaynova, E., Chernenko, G., Egorova, E., Zernitskaia, C., Manokhin, S., Tokmacheva-Kolobova, A., 2021. Laser-assisted fabrication and in vitro verification of functionalized surface for cells biointegration. Opt. Laser Technol. 1, (138) 106871.

Wang, J.H., Grood, E.S., Florer, J., et al, 2000. Alignment and proliferation of MC3T3-E1 osteoblasts in microgrooved silicone substrate subjected to cyclic stretching. J. Biomech. 33, 729.

Wang, D., Liao, X., Qin, X., Shi, W., Zhou, B., 2013. A novel chimeric peptide binds MC3T3-E1 cells to titanium and enhances their proliferation and differentiation. Mol. Med. Rep. 7 (5), 1437–1441.

Wilson, C.J., Clegg, R.E., Leavesley, D.I., et al, 2005. Mediation of biomaterial-cell interactions by adsorbed proteins: a review. Tissue Eng. 11, 1.

Xu, Z., Jiang, X., 2022. The promoting effect of the TiO2 nano-porous arrays after polydopamine-based modification and Arg-Gly-Asp peptide immobilization on biomineralization and osteogenesis. Ceram. Int. 48 (24), 37299–37309.

Xu, X., Wang, H., Zhang, S., Mei, X., Ying, B., Li, R., Qin, Y., 2022. ECM-inspired 3D printed polyetherimide scaffold with Arg-Gly-Asp peptides for the improvement of bioactivity and osteogenic differentiation of osteoblasts. Mat Today Com. 30, 103166.

Zheng, Q., Mao, L., Shi, Y., Fu, W., Hu, Y., 2022. Biocompatibility of Ti-6Al-4V titanium alloy implants with laser microgrooved surfaces. Mater. Technol. 37 (12), 2039–2048.

Zhou, L., Wu, J., Wu, D., Yu, J., 2019. Surface functionalization of titanium with BMP-7/RGD/hyaluronic acid for promoting osteoblast functions. J. Biomater. Tissue Eng. 9 (1), 32–39.